Post-Fire Vegetation (Non-)Recovery across the Edges of a Wildfire: An Unexplored Theme

Ivo Rossetti [1], Giulia Calderisi [2], Donatella Cogoni [2] and Giuseppe Fenu [2,*]

[1] Research Centre of S. Teresa, ENEA (Italian National Agency for New Technologies, Energy and Sustainable Economic Development), 19032 Lerici, Italy; ivo.rossetti@enea.it

[2] Department of Life and Environmental Sciences, University of Cagliari, 09123 Cagliari, Italy; giulia.calderisi@unica.it (G.C.); d.cogoni@unica.it (D.C.)

* Correspondence: gfenu@unica.it

Abstract: Wildfires have a significant influence on ecosystems globally, shaping vegetation, biodiversity, landscapes, soil properties, and other ecosystem processes. Despite extensive research on different aspects of wildfires, the edges of burned areas remain understudied, even though they involve complex dynamics. In this study, we analyzed the post-fire vegetation recovery across the edges of a large wildfire in a Mediterranean area. The investigations were focused on patches of woodlands that, in a previous study, showed a normalized burn ratio (NBR) decline one year after the fire. Field vegetation surveys were carried out in areas characterized by different NBR recovery rates and in areas outside the burned area as controls. Five hypotheses were tested, identifying delayed tree mortality as a key factor linked to NBR decline, particularly in low-severity fire zones in proximity to the fire edges. Delayed mortality, observed predominantly near the edges, may also affect unburned or less severely burned patches within the main fire perimeter, highlighting the need for ongoing monitoring. As these areas play a crucial role in the post-fire succession and vegetation dynamics, understanding the second-order effects of a fire is imperative for effective ecosystem management. This study underscores the importance of the long-term assessment of fire impacts, emphasizing the necessity of field surveys alongside remote sensing. Continued observation is essential to elucidate the enduring impacts of wildfires and to facilitate informed restoration strategies.

Keywords: delayed mortality; Montiferru; NBR; Sardinia; NBR decline; megafire; Mediterranean Basin

1. Introduction

Wildfires are among the most important disturbance factors affecting ecosystems and landscapes in many areas of the world [1–4]. Wildfires can exert both positive and negative effects on the vegetation structure and composition, biodiversity, carbon stocks, soil properties, hydrological processes, and ecosystem services [5,6].

In fire-prone regions, such as the Mediterranean Basin, vegetation has evolved for millennia under the pressure of recurrent fires, often set by humans in order to clear land for agriculture and farming [7–9]. Consequently, vegetation has developed effective strategies to cope with fires, such as basal resprouting from surviving below-ground organs, epicormic resprouting, and the germination of fire-resistant seeds [10–15]. Many Mediterranean landscapes are the result of a very long history of human-induced periodical fires, as well as selective deforestation and grazing activities, resulting in complex mosaics of agro-sylvo-pastoral ecosystems that are also recognized for their natural value [7–9,16].

In the last few decades, wildfire events have increased in frequency and severity because of global warming and land abandonment [15,17,18]. As a consequence, large wildfires are becoming more frequent also in the Mediterranean Basin [17–21].

Through the years, many efforts have been dedicated to investigating different aspects of wildfires. Concurrently with the progress of remote sensing techniques and the

availability of satellite imagery, noteworthy interest has been seen in the development and application of spectral indices to define, among other aspects, burned areas, fire severity, and post-fire vegetation recovery, e.g., [22–25]. However, most of the studies are focused on the inner parts of burned areas, while the edges are generally neglected. In fact, it is especially at the edges of the burned area that a number of complications and dynamics group together.

First of all, defining the edge of the burned area is difficult because of technical restrictions. Especially in large wildfires, remote sensing techniques are indispensable to quickly map the perimeters of burned areas and define the heterogeneity in the fire severity levels and post-fire vegetation recovery. However, these techniques have some drawbacks linked to the image resolution, the limitations of the spectral indices, and possible errors in multispectral sensors; low-resolution images lead to the less reliable estimation of the fire perimeter and the area burned [22,23]. Spectral analyses can be affected, among other factors, by the angles of illumination, shadowing, and the vegetation phenology [26–28], although many errors are amenable to mitigation or elimination. Generally, in proximity to burned areas' edges, the fire severity is low or moderate [29–31]. Therefore, the lower severity of the fire along the edges makes it more challenging to correctly define the perimeter of the burned area, because the spectral differences with the surrounding unburned vegetation are less manifest [28]. The same applies to the boundaries between moderate and high severity levels, because moderate severity is often circumscribed in narrow belts surrounding high-severity areas, making it more difficult to correctly define the limits of the belts affected by a moderate severity, especially when using low-resolution images [22]. Machine learning techniques, such as random forest methods, using a combination of medium-spatial-resolution (e.g., Sentinel-2) and high-spatial-resolution imagery (e.g., GF series, WorldView-2), can substantially enhance the classification accuracy for low- and moderate-severity fires [32]; however, it is not always possible to obtain high-resolution imagery, especially due to the associated costs and in cases of low-funded research. Low severity is often associated with sub-canopy burns, i.e., a fire that burns only the phytomass underneath the tree canopy. In the case of sub-canopy burns, multispectral sensors on satellites or aerial vehicles cannot detect spectral changes under a dense canopy layer; therefore, this eventuality, which can occur at the edges of a fire, can lead to the misinterpretation of the fire perimeter and fire severity [28]. Low and moderate severity have the lowest values of accuracy when estimated by remote sensing techniques [23]. Moreover, spectral indices can be misled by differences in moisture content in vegetation between pre-fire and post-fire scenes, thus under- or overestimating the burned area and fire severity [33]. In order to reduce these types of errors, combining remote sensing with field surveys is strongly recommended [26,33]. However, it is not always easy to obtain a representative number of sampling sites and walk through uneven, steep, and often dangerous areas to reach the locations of interest. This is especially true for large fires and mountainous regions.

Secondly, the edges of wildfires host a complex of mechanisms that involve species, communities, the ecosystem structure, and processes and also affect the landscape ecology level. Edges and their ecotones are important elements of contact among different ecosystems, and they can be generated by natural boundaries or disturbance factors, such as forest clearing and fires. After a fire, the edge of the burned area creates a new boundary between burned and unburned vegetation, which affects plant species and the communities and vegetation dynamics both on the burned and unburned sides through regeneration and mortality processes, competition, changes in species composition, resource availability, microclimatic effects, changes in soil physicochemical properties, and duff and seed bank removal due to smoldering [6,29,30,34]. Low- and moderate-severity fires are often accompanied by delayed tree mortality in injured trees. This type of vegetation dynamic, triggered by fires, can lead to the loss of large portions of phytomass, even for several years following fire extinction. As the fire severity near the edges of a wildfire is generally lower, delayed mortality can often occur across the fire perimeters [35]. The unburned sides of

fire edges are also important as refugia for flora and fauna; thus, they play an important role during the wildlife reestablishment process in burned areas [30,36].

The abovementioned aspects pertain also to the unburned islands within the fire perimeter, which are important as fire refugia, seed sources, recolonization areas, and habitat patches and contribute to the ecological complexity of the post-fire landscape [37–39].

For all of these reasons, it is important to analyze the dynamics at the edges generated by wildfires as well. Studies devoted to fire edges that are considered as references for this research are as follows: Harper and collaborators [30], who studied how the forest and landscape structure and composition are affected by fire edges in a black spruce boreal forest; Greene and collaborators [29], who studied how the distance from the fire edges affects seedbeds in boreal mixed woods; Diffendorfer and collaborators [36], who analyzed the role of the distance from the fire perimeter on the recovery of small mammals in chaparral; and, finally, several authors [28,35,37,39] who have studied the patterns and factors pertaining to the small unburned islands within the fire perimeter. To our knowledge, there are no or very few studies devoted to post-fire vegetation recovery at the edges of wildfires.

In our previous study [16], vegetation recovery one year after a fire event was analyzed using remote sensing techniques and field vegetation surveys in a Mediterranean area struck by a large wildfire in 2021. Spectral recovery was assessed by using the differenced normalized burn ratio (dNBR), applied to imagery from the Copernicus Sentinel-2 satellite mission, and comparing the post-fire scene with the scene one year after the fire. Our results indicated that the vegetation recovery was generally good, but the dNBR index highlighted areas showing low NBR recovery that also included patches of NBR decline. These areas appeared to be more related to woodlands and low- and moderate-severity fires and were mainly located near the edges of the burned area, also including the edges of unburned islands within the main fire perimeter.

As a consequence, in this study, we sought to investigate these areas, in order to understand the dynamics that generated them. Five hypotheses were tested to determine the causes of the identified areas: (i) delayed mortality, (ii) vegetation recovery failure, (iii) remote sensing errors, (iv) post-fire erosion phenomena, and (v) post-fire cleanup operations. Field surveys were carried out in woodlands at a significant number of sampling plots following the gradients of NBR recovery across the edges of the burned area in order to collect data to test the hypotheses.

2. Materials and Methods

2.1. Study Area

The study area (40°17′/40°6′ N-8°28′/8°42′ E) was located in Sardinia (Italy), within the historical region of Montiferru (Figure 1). In 2021, between the 23rd and 28th of July, the area was struck by a large wildfire that affected an area of 12,235.5 ha [16]. It was the largest wildfire in Italy in 2021 and one of the largest in the Mediterranean Basin in the same year. According to Linley and collaborators [40], such an event should be defined as a "megafire"; however, the use of this definition has recently been challenged as an ambiguous and emotive term that exaggerates the language used to describe fires [41] and was, therefore, not adopted in this study.

Geologically, the area is characterized by a massif of volcanic origin dating back to the Plio-Pleistocene, surrounded by a large coeval volcanic plateau. The rocks are composed of rhyolites and phonolites with trachybasalt dykes, alkaline and hawaiite basalts, and lava flows of alkaline and transitional basalts [42]. The altitude of the study area ranges from 10 m above sea level to 1050 m at the highest peak of the Montiferru massif. The mean annual temperatures range from 8.8 °C in January to 24.6 °C in August, and the mean annual rainfall amounts to 739.3 mm. The bioclimate is Mediterranean pluviseasonal oceanic, with upper thermo-Mediterranean to upper meso-Mediterranean belts, and upper dry to lower humid, according to the Rivas-Martinez classification system [43].

The landscape consists of an agro-sylvo-pastoral system characterized by a complex mosaic of land uses and vegetation types. Semi-natural grasslands, mainly consisting of semi-natural plant communities, and fodder crops cover almost half of the area. These land uses represent the main matrix of the landscape and are related to extensive livestock farming. Before the wildfire, woodlands dominated by *Quercus ilex* L. and *Q. suber* L. and, secondarily, by deciduous oaks, covered 20% of the study area. Mediterranean shrublands were also widespread, covering 16% of the area. Cultivation, reforestation, urban areas, infrastructure, and other anthropized areas occupied 15% of the study area [44].
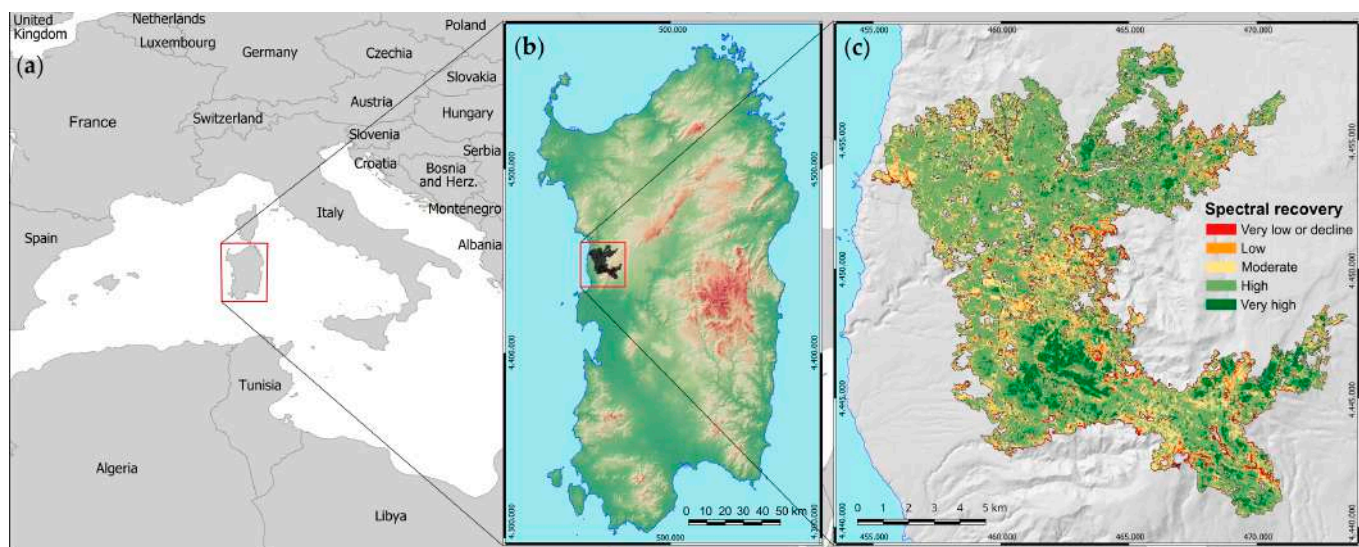
Figure 1. Map of the study area. (**a**) Location of Sardinia (Italy). (**b**) Map of Sardinia with the location of the area struck by the wildfire in 2021. (**c**) Map of the spectral recovery levels (based on dNBR) one year after the fire. The areas colored in red, i.e., the patches with very low NBR recovery or NBR decline, are the areas of interest in this study. The reference system is WGS84–UTM.

2.2. Preliminary Analyses and Background

We observed that the areas of interest were mainly related to woodlands and appeared to be mostly located close to the edges of the burned area, where the fire struck with very low to moderate severity. Hence, prior to undertaking the investigations to explain these low-recovery areas, preliminary analyses were carried out to verify the above-mentioned observations.

The raster map of spectral recovery one year after the fire [16] was used to extract the burned areas that showed very low NBR recovery and NBR decline. The raster map, with a spatial resolution of 10 m, was elaborated from the Copernicus Sentinel-2 multispectral data by using the normalized burn ratio (NBR) and differenced normalized burn ratio (dNBR) as spectral indices. These indices use the reflectance in the near-infrared (NIR) and short-wave infrared (SWIR) bands. By using these bands, the NBR and dNBR indices were calculated as follows:

$$NBR = (NIR - SWIR)/(NIR + SWIR), \tag{1}$$

$$dNBR_{post\text{-}1yr} = NBR_{post\text{-}fire} - NBR_{1yr}, \tag{2}$$

where $NBR_{post\text{-}fire}$ is the NBR calculated on the satellite image acquired after the fire's extinction, and NBR_{1yr} is the NBR calculated on the images acquired one year after the fire extinction date. $dNBR_{post\text{-}1yr}$ gives an estimation of the vegetation recovery one year after the fire. Since healthy vegetation reflects more in the NIR region and less in the SWIR region [23], vegetation recovery leads to higher values of NBR_{1yr}. Therefore, negative values of $dNBR_{post\text{-}1yr}$ are evidence of vegetation regrowth. Conversely, positive values may indicate vegetation regrowth failure or possible phytomass loss (Table 1). Cloudless

Sentinel-2 images [45] with sensing dates of 30 July 2021 and 1 August 2022 were utilized to compute $dNBR_{post-1yr}$.

Table 1. Meaning of $dNBR_{post-1yr}$ values (scaled by 1000) as recovery levels. The recovery level thresholds for low, moderate, high, and very high are based on the severity classification proposed by the European Forest Fire Information Service [46]. For the unrecovered/very low and decline levels, the thresholds are based on Key and Benson (2006) [33].

$dNBR_{post-1yr}$ Values	Recovery Level	Meaning
$dNBR \geq +100$	Decline	Phytomass loss
$+99 \geq dNBR \geq -100$	Unrecovered/Very low	Little or no change
$-101 \geq dNBR \geq -255$	Low	
$-256 \geq dNBR \geq -419$	Moderate	Vegetation regrowth
$-420 \geq dNBR \geq -660$	High	
$dNBR < -660$	Very high	

Consequently, the zones showing very low recovery and a decline one year after the fire were extracted by selecting all pixels with $dNBR_{post-1yr}$ values between -100 and the maximum positive value ($+572$ in our case study). The extracted zones were classified into woodlands, shrublands, and semi-natural grasslands on the basis of the regional land use map [44] and updated through field inspections and the observation of recent orthophotos; then, their areas were calculated and expressed as a percentage of the total burned area of each type of vegetation.

In order to assess whether the zones showing very low recovery and declines were mainly related to woodlands, the pixel values of $dNBR_{post-1yr}$ were sampled at points randomly projected with a density of 25 points per ha and a 15 m minimum distance among points to avoid using more than one point per pixel. A total of 6763 points were projected (4769 for woodlands, 1276 for shrublands, and 718 for grasslands). The homogeneity of variance was assessed using Levene's test; then, the nonparametric Kruskal–Wallis test and Dunn's post hoc comparisons were performed to test for statistical differences.

To assess whether the zones showing very low recovery and declines were mostly located close to the edges of the burned area, the pixel values of $dNBR_{post-1yr}$ were sampled at points randomly projected inside the whole burned area, at distances of between 0 and 100 m from the fire perimeter. The points were projected with a density of 1 point per ha and a 50 m minimum distance among points. A total of 5420 points were projected (820 for woodlands, 976 for shrublands, and 3624 for grasslands). The nonparametric Spearman's rank correlation coefficient (*rho*) between the values of $dNBR_{post-1yr}$ and the distance from the fire perimeter was used to test the null hypothesis. The test was performed overall and for woodlands, shrublands, and grasslands separately.

All cartography computations were performed in QGIS, version 3.28 [47]. Statistical tests were conducted in JASP, version 0.18.1 [48].

2.3. Experimental Design

To explain the lack of NBR recovery one year after the fire, five hypotheses were formulated.

1. Delayed mortality: areas showing very low NBR recovery and NBR decline may have been affected by delayed mortality, i.e., tree or shrub mortality that started with the fire but occurred at a later time. It mainly affects older trees and fire-resistant species such as *Quercus* species [3]. Delayed mortality leads to phytomass loss; therefore, it could explain the NBR decline (i.e., positive values of $dNBR_{post-1yr}$).

2. Vegetation recovery failure: The vegetation regrowth process may have failed in the areas that showed very low NBR recovery and NBR decline.

3. Remote sensing errors: The satellite sensor may not have detected some areas that were actually affected by the fire. This can occur, for example, in the case of sub-canopy burn, i.e., when a fire burns only the phytomass underneath dense tree canopy

cover [28]. In this case, the satellite sensor cannot detect spectral changes under the tree canopy; therefore, the calculation of the burn severity and NBR recovery could have been affected by these errors.

4. Post-fire erosion: Soil runoff or landslide events that may have occurred after the fire could have led to the loss of vegetation cover or plant death, thus affecting the signal of NBR recovery.

5. Post-fire cleanup operations: Forest fire cleanup operations after fire extinction, such as the removal of hazardous trees or flammable vegetation near the perimeter of the burned area to avoid reignition, could have led to phytomass loss; therefore, they may have affected the signal of NBR recovery.

In order to test these hypotheses, vegetation surveys were conducted in the field in woodlands under four different conditions: burned woodlands that showed very low NBR recovery or NBR decline, collectively called no-recovery areas (NR); burned woodlands that showed high or very high NBR recovery (HR); woodlands outside the burned area but very close to the edges of NR areas (EDG); and unburned woodlands (UNB). EDG and UNB sites were included in the experiment as controls.

The study sites were located using the QGIS software, version 3.28 [47]. NR woodland sites were identified as described in the previous paragraph. HR sites were identified in areas showing high and very high NBR recovery levels within a 100 m buffer zone around NR sites, in order to minimize the differences due to the spatial distance. EDG sites were located no more than 20 m outside the perimeter of the burned area, but within 50 m from NR sites. UNB sites were located in unburned woodlands at least 100 m away but not more than 200 m from the perimeter of the fire, also in this case to minimize the differences due to the spatial distance.

This experimental design allowed us to cross the gradients at the edges of the burned area, starting from high NBR recovery areas, passing through areas showing low NBR recovery and NBR decline next to the edges of the burned area, and then moving on to areas directly outside the burned area and finally to areas not affected by the fire.

Random points were projected with a density of 1 point per ha and a 50 m minimum distance among points inside the identified areas in order to locate the sampling plots in the field (Figure S1).

2.4. Field Surveys

The mapped points were reached in the field using a GPS and Galileo receiver, the Garmin® Montana® 750i. At each point, a rectangular plot of approximately 200 m^2 was identified as the sampling area. The size of the sampling area was chosen to ensure that it was large enough to comprehensively consider the structural and compositional aspects of the forest vegetation under investigation. The shape of the sampling area was chosen to be rectangular (approximately 10 m × 20 m) to avoid possible overlaps with adjacent areas having different NBR recovery levels. A 200 m² sampling area approximately corresponded to 2 pixels on the NBR recovery map.

At each sampling area, the following information was collected: the cover percentage and height of new sprouts related to basal resprouting and seed germination (Cover$_{sprouts}$ and Height$_{sprouts}$); the cover percentage and height of plants that survived the fire (Cover$_{survived}$ and Height$_{survived}$); the percentage of living plants unaffected by the fire, separately for the tree and shrub layers (Living unburned$_{trees}$ and Living unburned$_{shrubs}$); the percentage of living trees and shrubs affected by the fire, separately for the tree and shrub layers (Living burned$_{trees}$ and Living burned$_{shrubs}$); the percentage of dead plants affected by the fire, separately for the tree and shrub layers (Dead burned$_{trees}$ and Dead burned$_{shrubs}$); the percentage of plants that survived the fire or were apparently unaffected by the fire but died at a later time, separately for the tree and shrub layers (Delayed mortality$_{trees}$ and Delayed mortality$_{shrubs}$); the presence or absence of clear evidence of post-fire erosion phenomena; and the presence or absence of post-fire cleanup operations, such as the human-mediated cutting of trees or removal of strips of vegetation.

In order to distinguish between plants immediately killed by the fire and those affected by delayed mortality, the general state of the plants was evaluated. Plants totally charred and bare were considered immediately killed by the fire, while plants with no blackened stems and branches, or those slightly affected by the fire but showing recently dead leaves, were considered plants affected by delayed mortality. Moreover, it is important to state that only the above-ground parts of the plants were considered to measure the parameters listed above; therefore, the percentages related to dead plants must be considered as measures of top killing (i.e., when the fire kills the above-ground portion of a plant).

Given the operational difficulties in the field, each survey was conducted by at least three surveyors and the values reported are the averages of the evaluations of the three surveyors. Overall, 176 plots were surveyed (44 plots for each condition). Surveys were carried out in late spring 2023, once deciduous plants had already developed their leaves, in order to ensure that the vegetation was at the maximum development stage.

2.5. Hypothesis Testing and Data Analysis

To test hypothesis 1 (delayed mortality), the percentages of trees and shrubs that died at a later time after the fire were used as variables (Delayed mortality$_{trees}$ and Delayed mortality$_{shrubs}$). If NR plots were linked to delayed mortality, then the median value should be significantly higher than in HR plots.

The cover and height of the surviving aerial parts of vegetation (Cover$_{survived}$ and Height$_{survived}$) and the cover and height of new sprouts by basal resprouting and seed germination (Cover$_{sprouts}$ and Height$_{sprouts}$) were used as variables to test hypothesis 2 (vegetation recovery failure). If NR plots were linked to vegetation recovery failure, then the median values should be significantly lower than in HR plots.

To test hypothesis 3 (remote sensing errors), six variables were considered: the percentages of living unburned trees and shrubs (Living unburned$_{trees}$ and Living unburned$_{shrubs}$), the percentages of living burned trees and shrubs (Living burned$_{trees}$ and Living burned$_{shrubs}$), and the percentages of dead burned trees and shrubs (Dead burned$_{trees}$ and Dead burned$_{shrubs}$). If NR plots were linked to remote sensing errors, then the median values should be significantly different from those in HR plots. Moreover, in the case of sub-canopy burns, only the shrub layer should manifest burned plants.

Hypotheses 4 and 5 were tested by comparing the number of NR and HR plots where erosion phenomena or signs of post-fire cleanup operations were observed in order to determine if a relationship existed with NR plots.

After testing the homogeneity of variance using Levene's test, the nonparametric Kruskal–Wallis test and Dunn's post hoc comparisons were performed to test hypotheses 1, 2, and 3. Bonferroni correction was applied to the post hoc comparisons to obtain more conservative *p* values. For hypothesis 3, to verify the incidence of sub-canopy burns in the plots next to the edges of the burned area (i.e., NR and EDG plots), a logistic regression model was applied in order to ascertain whether the tree canopy and shrub layer affected by the fire were associated or not. The chi-square (χ^2) test for independence was used to test hypotheses 4 and 5 and to determine whether the plots affected by the fire (NR and HR plots) were associated with post-fire erosion events. Analyses were performed in JASP version 0.18.1 [48].

3. Results

One year after the wildfire, areas showing very low NBR recovery and NBR decline amounted to 384.4 ha, which corresponded to 3.14% of the total burned area (12,235.5 ha).

In burned woodlands, 195.9 ha out of 1958.6 ha (i.e., 10%) showed very low NBR recovery and NBR decline one year after the fire. As regards other types of seminatural vegetation, 56.8 ha out of 2394.0 ha (i.e., 2.37%) of burned shrublands and 37.4 ha out of 6009.0 ha of burned grasslands (0.6%) were unrecovered one year after the fire. The remaining spectrally unrecovered areas were related to reforested, cultivated, anthropized, and sparsely vegetated areas.

Comparing the dNBR$_{post-1yr}$ values of unrecovered areas, the non-parametric Kruskal–Wallis test and Dunn's post hoc comparisons showed highly significant differences ($p < 0.001$) among woodlands, shrublands, and grasslands. The spectrally unrecovered woodlands showed higher dNBR$_{post-1yr}$ values than in shrublands and grasslands (Figure 2).

Figure 2. Boxplots and violin plots of dNBR$_{post-1yr}$ values in the areas showing very low NBR recovery and NBR decline one year after the fire in grasslands, shrublands, and woodlands. The boxes show the interquartile range, the horizontal bars show median values, and the vertical bars show the top and bottom 25% quartiles. The violin plots display the distribution curves of the dNBR$_{post-1yr}$ values. Median values with different lowercase letters significantly differ at $p < 0.05$.

As shown by the Spearman's rank correlation coefficients, the values of dNBR$_{post-1yr}$ were inversely correlated with the distance from the edges of the burned area (Table 2). The correlation was stronger for woodlands. All Spearman's rank correlation coefficients were highly significant ($p < 0.001$). Woodlands, compared to shrublands and grasslands, exhibited more positive dNBR$_{post-1yr}$ values at a shorter distance from the edges of the burned area (Figure 3).
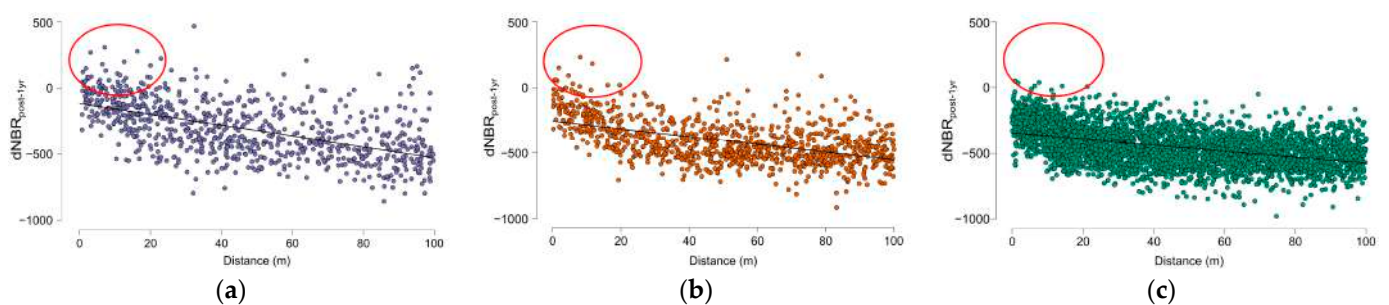
Figure 3. Scatterplots of the correlations between the dNBR$_{post-1yr}$ values and distances from the edges of the burned area for (**a**) woodlands, (**b**) shrublands, and (**c**) grasslands. Red circles highlight the areas of the plots with the highest dNBR$_{post-1yr}$ values at a shorter distance from the edges of the burned area.

Table 2. Spearman's rank correlation coefficients (*rho*).

dNBR$_{post-1yr}$–Distance Correlation	Spearman's *rho*
Overall	−0.477 ***
Woodlands	−0.590 ***
Shrublands	−0.504 ***
Grasslands	−0.474 ***

*** $p < 0.001$.

3.1. Test of Hypothesis 1: Delayed Mortality

The Kruskal–Wallis test indicated highly significant differences ($p < 0.001$) among the conditions in terms of delayed mortality in the tree layer. The Dunn's post hoc comparisons showed highly significant differences ($p < 0.001$) between NR and HR plots, NR and EDG plots, and NR and UNB plots. Conversely, no significant differences were found among other comparisons ($p > 0.05$; see Table S1—Supplementary Materials, for the *p* values of all comparisons). The median percentage of dead unburned trees in NR (20%) was significantly higher than in other conditions, where the median percentage was 0% (Figure 4a).
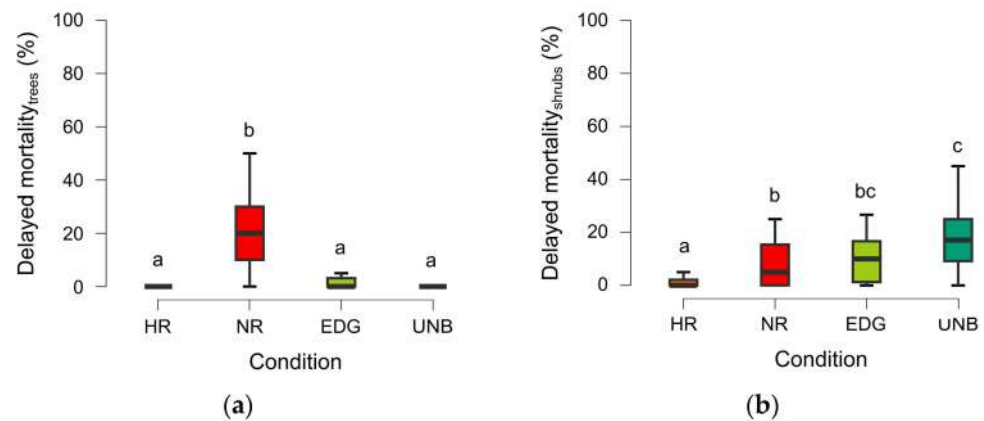

Figure 4. Boxplots of (**a**) percentage of trees and (**b**) percentage of shrubs affected by delayed mortality in high NBR recovery plots (HR), no NBR recovery plots (NR), edge plots (EDG), and unburned (UNB) plots. The boxes show the interquartile range, the horizontal bars show median values, and the vertical bars show the top and bottom 25% quartiles. Median values with different lowercase letters significantly differ at $p < 0.05$.

The Kruskal–Wallis test indicated highly significant differences ($p < 0.001$) among the conditions for the shrub layer as well. The Dunn's post hoc comparisons showed significant differences ($p < 0.05$) among the conditions, except between HR and NR plots and EDG and UNB plots ($p > 0.05$; Table S1—Supplementary Materials). The median percentage of dead unburned shrubs in HR (0%) was significantly different from that in NR (5%) and EDG plots (10%); HR significantly differed from UNB plots (17%), while EDG and UNB plots were not significantly different from each other (Figure 4b).

3.2. Test of Hypothesis 2: Vegetation Recovery Failure

The Kruskal–Wallis test indicated highly significant differences ($p < 0.001$) among the conditions for the cover of sprouts. The Dunn's post hoc comparisons showed significant differences ($p \leq 0.001$) among the conditions, except between HR and NR ($p > 0.05$; Table S2—Supplementary Materials). The median cover of sprouts in NR (15%) and in HR (20%) was significantly higher than in EDG and UNB plots (Figure 5a). EDG plots showed low median cover of sprouts (5%), but it was significantly higher than in UNB plots, where sprouts were absent (Figure 5a).

(**a**)

(**b**)
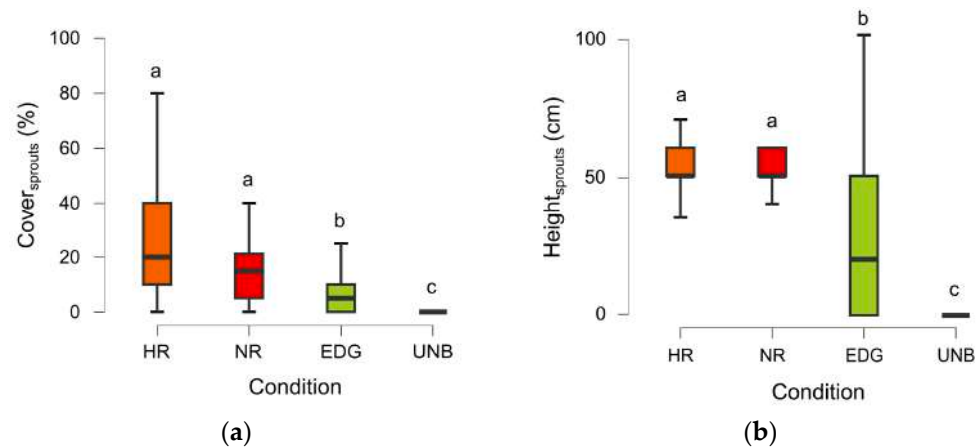
Figure 5. Boxplots of (**a**) cover and (**b**) height of sprouts in high NBR recovery plots (HR), no NBR recovery plots (NR), edge plots (EDG), and unburned plots (UNB). The boxes show the interquartile range, the horizontal bars show median values, and the vertical bars show the top and bottom 25% quartiles. Median values with different lowercase letters significantly differ at *p* < 0.05.

Likewise, the height of sprouts, according to the Kruskal–Wallis test, showed highly significant differences (*p* < 0.001) among the conditions. The Dunn's post hoc comparisons showed highly significant differences (*p* < 0.001) among the conditions, except between HR and NR (*p* > 0.05; Table S2—Supplementary Materials). The median height of sprouts in NR (50 cm) and HR (55 cm) significantly differed from those in EDG and UNB plots (Figure 5b). EDG plots showed a median sprout height of 20 cm, which was significantly higher than in UNB plots, where sprouts were absent (Figure 5b).

In terms of the cover of surviving plants, the Kruskal–Wallis test indicated highly significant differences (*p* < 0.001) among the conditions. The Dunn's post hoc comparisons showed significant differences (*p* ≤ 0.001) among the conditions, except between HR and NR (*p* > 0.05; Table S3—Supplementary Materials). The median cover of surviving plants in NR (25%) was lower than in HR (50%), but this difference was not significant (Figure 6a). On the other hand, the median cover of surviving plants in HR and NR was significantly lower than in EDG and UNB plots. EDG plots showed the high median cover of surviving plants (80%), but it was significantly lower than in UNB plots (95%; Figure 6a).
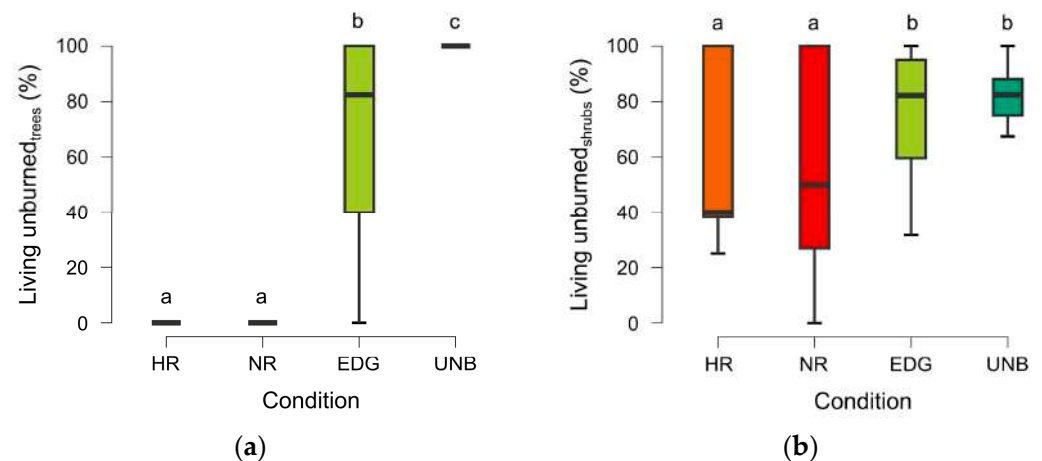

(**a**)

(**b**)
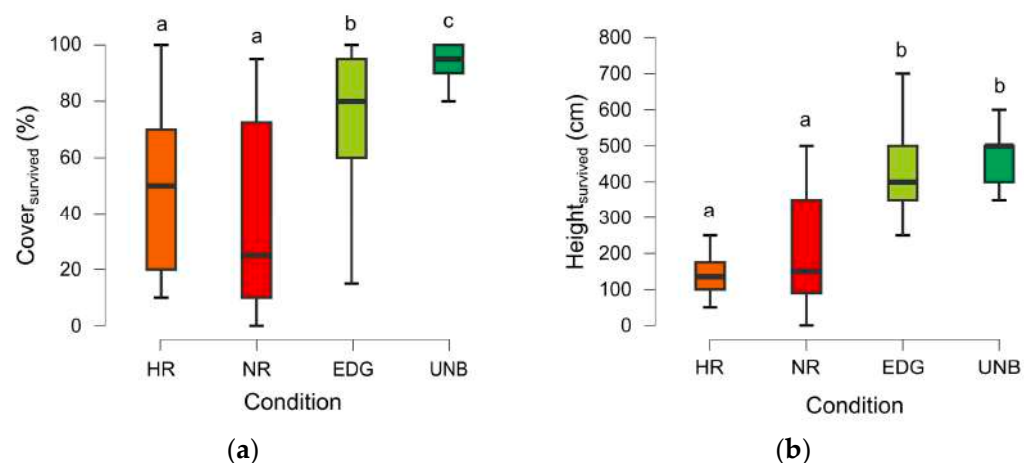
Figure 6. Boxplots of (**a**) cover and (**b**) height of surviving plants in high NBR recovery plots (HR), no NBR recovery plots (NR), edge plots (EDG), and unburned plots (UNB). The boxes show the interquartile range, the horizontal bars show median values, and the vertical bars show the top and bottom 25% quartiles. Median values with different lowercase letters significantly differ at *p* < 0.05.

Likewise, the height of surviving plants showed, according to the Kruskal–Wallis test, highly significant differences ($p < 0.001$) among the conditions. Accordingly, the Dunn's post hoc comparisons showed highly significant differences ($p < 0.001$) among the conditions, except between HR and NR plots and between EDG and UNB plots ($p > 0.05$; Table S3—Supplementary Materials). The median height of surviving plants in NR (150 cm) and HR (135 cm) significantly differed from those in EDG (400 cm) and UNB plots (500 cm; Figure 6b).
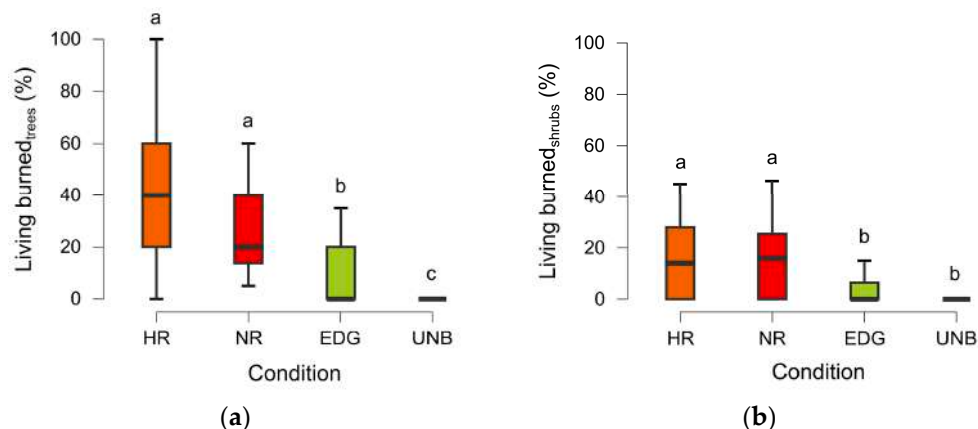
3.3. Test of Hypothesis 3: Remote Sensing Errors

The Kruskal–Wallis test indicated highly significant differences ($p < 0.001$) among the conditions for the percentage of living unburned trees. The Dunn's post hoc comparisons showed significant differences ($p < 0.01$) among the conditions, except between HR and NR ($p > 0.05$; Table S4—Supplementary Materials). The median percentages of living unburned trees in NR and HR (0%) were significantly lower than in EDG and UNB plots (82.5% and 100%, respectively; Figure 7a); the difference between EDG and UNB plots was also significant (Figure 7a).

Figure 7. Boxplots of (**a**) percentage of living unburned trees and (**b**) percentage of living unburned shrubs in high NBR recovery plots (HR), no NBR recovery plots (NR), edge plots (EDG), and unburned plots (UNB). The boxes show the interquartile range, the horizontal bars show median values, and the vertical bars show the top and bottom 25% quartiles. Median values with different lowercase letters significantly differ at $p < 0.05$.

The Kruskal–Wallis test indicated highly significant differences ($p < 0.001$) among the conditions for the percentage of living unburned shrubs. The Dunn's post hoc comparisons showed significant differences ($p < 0.05$) among the conditions, except between HR and NR and between EDG and UNB plots ($p > 0.05$; Table S4—Supplementary Materials). The median percentages of living unburned shrubs in NR (50%) and HR (40%) were significantly lower than in EDG and UNB plots (82.25% and 82.5%, respectively; Figure 7b).
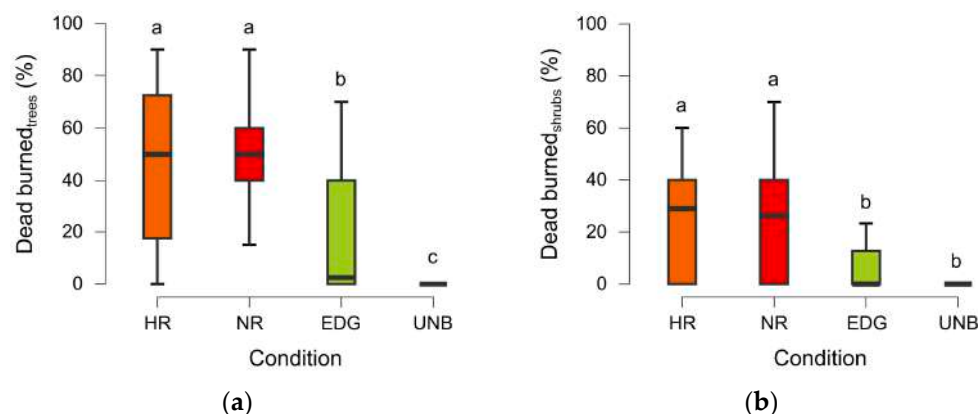
The Kruskal–Wallis test indicated highly significant differences ($p < 0.001$) among the conditions in the percentage of living burned trees. The Dunn's post hoc comparisons showed significant differences ($p < 0.01$) among the conditions, except between HR and NR ($p > 0.05$; Table S5—Supplementary Materials). The median percentages of living burned trees in NR (20%) and HR (40%) were significantly higher than in EDG and UNB plots; the difference between EDG and UNB plots was also significant (Figure 8a).

Figure 8. Boxplots of (**a**) percentage of living burned trees and (**b**) percentage of living burned shrubs in high NBR recovery plots (HR), no NBR recovery plots (NR), edge plots (EDG), and unburned plots (UNB). The boxes show the interquartile range, the horizontal bars show median values, and the vertical bars show the top and bottom 25% quartiles. Median values with different lowercase letters significantly differ at $p < 0.05$.

The Kruskal–Wallis test indicated highly significant differences ($p < 0.001$) among the conditions for the percentage of living burned shrubs. The Dunn's post hoc comparisons showed highly significant differences ($p < 0.001$) among the conditions, except between HR and NR plots and EDG and UNB plots ($p > 0.05$; Table S5—Supplementary Materials). The median percentages of living burned shrubs in NR (15.83%) and HR (14%) were significantly higher than in EDG and UNB plots (Figure 8b).

The Kruskal–Wallis test indicated highly significant differences ($p < 0.001$) among the conditions for the percentage of dead burned trees. The Dunn's post hoc comparisons showed highly significant differences ($p < 0.001$) among the conditions, except between HR and NR ($p > 0.05$; Table S6—Supplementary Materials). The median percentages of dead burned trees in NR (50%) and HR (50%) were significantly higher than in EDG (2.5%) and UNB plots (0%); the difference between EDG and UNB plots was also significant (Figure 9a).

Figure 9. Boxplots of (**a**) percentage of dead burned trees and (**b**) percentage of dead burned shrubs in high NBR recovery plots (HR), no NBR recovery plots (NR), edge plots (EDG), and unburned plots (UNB). The boxes show the interquartile range, the horizontal bars show median values, and the vertical bars show the top and bottom 25% quartiles. Median values with different lowercase letters significantly differ at $p < 0.05$.

The Kruskal–Wallis test indicated highly significant differences ($p < 0.001$) among the conditions for the percentage of dead burned shrubs. The Dunn's post hoc comparisons did not show significant differences between HR and NR or between EDG and UNB plots

(p > 0.05; Table S6—Supplementary Materials). The median percentages of dead burned shrubs in NR (26.25%) and HR (29%) were significantly higher than in EDG and UNB plots (0%; Figure 9b).

The logistic regression model, performed for NR and EDG plots (88 plots overall) to verify the incidence of sub-canopy burns next to the edges of the burned area, showed that a fire in the shrub layer was significantly associated with a fire in the tree layer (χ^2 = 15.214, p < 0.001), with an odds ratio of 12.0. Therefore, there was no significant incidence of sub-canopy burns. The model correctly classified 65.9% of cases.

3.4. Test of Hypotheses 4 and 5: Post-Fire Erosion and Post-Fire Cleanup Operations

Among the 88 plots considered to test these hypotheses (44 for NR and 44 for HR), only 13 presented signs of post-fire erosion (six in HR and seven in NR plots), while nine plots presented signs of post-fire cleanup operations (five in HR and four in NR plots).

The chi-squared test on contingency tables 2 × 2 did not show any significant association between the presence or absence of signs of erosion events or cleanup operations and HR–NR plots (Table 3).

Table 3. Chi-squared tests for NR plots vs. HR plots.

	Value	df	p
χ^2erosion events	0.090	1	0.764
χ^2cleanup operations	0.124	1	0.725
N	88		

When comparing all plots affected by the fire (i.e., NR and HR plots) with all plots outside the burned area (i.e., EDG and UNB plots), a highly significant association was found between plots affected by the fire and erosion events. On the other hand, no significant association was found with cleanup operations (Table 4).

Table 4. Chi-squared tests for NR and HR plots vs. EDG and UNB plots.

	Value	df	p
χ^2erosion events	14.037	1	<0.001
χ^2cleanup operations	3.220	1	0.073
N	176		

4. Discussion

In our study area, the incidence of the patches showing no NBR recovery was low if compared with the total burned area. However, considering the size of the burned surface, the total area showing no NBR recovery was relevant in absolute terms.

The comparisons among the vegetation types confirmed the prevalence of spectrally unrecovered areas in woodlands, both in terms of the area and dNBR$_{post-1yr}$ values. This was mostly due to the differences in the resilience of the three vegetation types considered, as the importance of the factors shaping the vegetation recovery dynamics in the short term after a fire is largely plant-community-dependent [49]. Grasslands are mostly composed of annual herbs, geophytes, and hemicryptophytes, which are usually fast-growing and have higher efficiency in their use of soil moisture, nutrient uptake, and carbon assimilation [50–54]. For these reasons, grasslands need less time to regain their original conditions with respect to other types of vegetation. Moreover, grasslands typically experience lower levels of fire severity [55,56]. Essentially, burned grasslands represented only 0.6% of the spectrally unrecovered areas. However, it has to be considered that, in the study area, grasslands were generally related to livestock farming; therefore, the NBR recovery one year after the fire could have been affected by grazing activities or other forms of land management. Consequently, the presence of areas showing no NBR recovery one

year after a fire in grasslands has to be mainly considered due to management activities and is not necessarily linked to the failure of vegetation recovery. In our study area, shrublands represented an intermediate stage of the vegetation dynamics, and they were characterized by high complexity in terms of their structure and floristic composition, which were developing towards the woodland type. For this reason, in terms of NBR recovery, shrublands showed an intermediate pattern between grasslands and woodlands.

The correlation between the $dNBR_{post-1yr}$ values and the distance from the fire perimeter confirmed that the areas showing no NBR recovery were mostly located close to the edges of the burned area. This correlation was stronger for woodlands, which also exhibited more positive $dNBR_{post-1yr}$ values. The possible reasons for these findings are various and will be discussed thoroughly in the following sections regarding the hypotheses tested in this study.

4.1. Delayed Mortality (Hypothesis 1)

The testing of hypothesis 1 showed strong evidence that NR plots were related to delayed mortality, especially in the tree layer. The percentage of trees that survived the fire but died afterward was significantly higher than in HR plots, which were similar to EDG and UNB plots instead. Mortality after the fire's extinction also affected the shrub layer. In fact, in NR plots, the percentage of shrubs that died later, after the fire, was significantly higher than in HR plots. The shrub layer in EDG plots showed higher delayed mortality than in NR plots, but this difference was not significant. UNB plots showed the highest delayed mortality in the shrub layer. However, the mortality of shrubs in UNB plots should not be attributed to the fire but to other types of stressors, such as competition, pests and pathogen activity, and drought [5,57]. These stressors can also be important in low- and mixed-severity fire regimes [5]; therefore, the observed delayed mortality of shrubs in NR and EDG plots could be related both to stress caused by the fire and other types of stressors. The strong competition from new shoots related to basal resprouting and seed germination may have led to the delayed mortality of shrubs already weakened by the fire.

The incidence of delayed tree mortality in NR plots may explain the positive values of $dNBR_{post-1yr}$, confirming that the positive values were likely related to the phytomass loss that occurred at a later time after the fire's extinction.

Supported by the statistical evidence of this study, hypothesis 1 can be accepted: NR areas were significantly linked to the delayed mortality of trees.

4.2. Vegetation Regeneration Failure (Hypothesis 2)

No evidence of lower vegetation recovery was highlighted in NR plots compared to HR ones. In terms of the cover and height of new sprouts by basal resprouting and seed germination, HR and NR plots appeared to be similar, suggesting that vegetation regrowth, in both conditions, proceeded at a similar pace. Likewise, no significant differences between HR and NR plots were detected regarding the cover and height of the surviving above-ground parts of plants, suggesting that the vegetation recovery did not differ in terms of epicormic resprouting either. Although NR plots showed lower median values for the cover of sprouts and the cover of surviving plants, these differences were not significant. For these reasons, hypothesis 2 cannot be accepted: NR areas were not linked to vegetation regeneration failure.

As expected, EDG and UNB plots, which were outside the burned area, had the lowest values for the cover and height of sprouts and the highest values for the cover and height of surviving plants. However, EDG plots showed values that were slightly but significantly different from those of UNB plots, suggesting that EDG plots were affected by the fire to some extent.

4.3. Remote Sensing Errors (Hypothesis 3)

Our results indicate that NR plots were not linked to errors in the computation of the burn severity and NBR recovery. In fact, no significant differences were highlighted

between NR and HR plots in terms of the percentages of living unburned, living burned, and dead burned trees and shrubs. Both the tree and shrub layers were affected by the fire, suggesting that there was no significant incidence of sub-canopy burns, leading to possible errors in the satellite sensor in detecting spectral changes. Therefore, hypothesis 3 cannot be accepted: NR areas were not linked to remote sensing errors.

The EDG and UNB plots were significantly different from the NR and HR ones. As expected, the percentage of living unburned plants in the plots outside the burned area was close to 100%. Conversely, the percentages of living burned and dead burned plants were close to zero. Nevertheless, as already observed (see Section 4.2), the EDG plots were found to be affected by the fire to some extent.

4.4. Post-Fire Erosion and Post-Fire Cleanup Operations (Hypothesis 4 and 5)

No evidence of associations between NR plots and post-fire erosion phenomena or post-fire cleanup operations was found. These circumstances were almost equally distributed between the NR and HR plots. Therefore, hypotheses 4 and 5 cannot be accepted: NR areas were not linked to post-fire erosion phenomena or post-fire cleanup operations.

On the other hand, erosion was preferentially associated with plots affected by the fire (NR and HR plots). Erosion phenomena were not at all found in EDG and UNB plots, suggesting that, in some areas, the lack of vegetation cover exposed the soil to a higher erosion risk. This evidence is consistent with a large body of literature, e.g., [6,58–60].

4.5. Vegetation Recovery Pattern across the Edges of the Wildfire

In this study, which focused mainly on Mediterranean woodlands, the correlation analysis between the $dNBR_{post-1yr}$ values and the distance from the fire perimeter revealed a notable association between the absence of NBR recovery and the proximity to the fire edges. This suggested that the vegetation recovery rates were lower in areas close to the fire perimeter, with woodlands experiencing a more substantial NBR decline during the first year post-fire. The delayed mortality hypothesis (Hypothesis 1), tested on field data, supports this observation, indicating a significant association between delayed tree mortality and spectrally declined areas. Delayed tree mortality detected in the field was generally associated with NR plots, which were closer to the edges of the burned area and were mostly affected by low-severity fires. On the other hand, delayed tree mortality was not detected in HR plots, which were further from the edges and mostly affected by high and very high severity.

The findings of this study need to be discussed in light of the effects that fires exert on plants, communities, and ecosystems. These effects can be classified as direct or first-order effects and indirect or second-order effects [2,5,61–63]. Direct effects are related to heat injuries directly caused by the fire to plant tissues and can affect all plant organs. Two main mechanisms are referred to as direct effects: cambium necrosis and hydraulic dysfunction [2,63]. In the case of high-severity fires, direct heat injuries can immediately kill the plant or, in the case of resprouting species, can kill only the above-ground portion of the plant (top killing) [5]. On the other hand, especially in low- and mixed-severity fires, the plant can survive the immediate effects of the fire. In this case, the plant has to face complex internal and external mechanisms that concern the physiology and ecology spheres. These mechanisms pertain to the indirect effects of a fire. The heat-induced impairments in the cambium, phloem, and xylem can lead, in the short or long term, to carbon starvation and hydraulic failure, which can make the plant more susceptible to drought, competition, and pathogen or insect attacks, which may also lead to delayed plant mortality [2,5,64]. The likelihood of a plant to survive a fire is also dependent on the pre-fire conditions, such as inter- or intraspecific competition, drought stress, pests, or diseases [5,64,65].

Considering the scarcity of studies concerning the post-fire vegetation dynamics across the edges of wildfires in the Mediterranean region, our outcomes can be compared with other studies carried out in different ecoregions. Reilly and collaborators [35], in fires that occurred in California, Washington, and Oregon, found that delayed tree mortality occurred

across fire perimeters not affected by stand-replacing fires. In fact, in stand-replacing fires, which are generally characterized by high severity, most of the above-ground phytomass is directly killed by the fire; therefore, delayed mortality is basically missing and vegetation recovery is based on basal resprouting and seed germination [5]. In proximity to the fire edges, the fire severity is generally lower [29–31]; therefore, there is a higher probability that a larger number of trees will survive the fire. However, the physiology of the surviving trees can be compromised, exposing them to detrimental delayed effects that may also lead to delayed death [2,66,67].

Summarizing the results, our case study was focused on the gradients of fire severity and NBR recovery across the edges of a burned area, starting from the areas showing high NBR recovery (HR), passing through areas showing no NBR recovery next to the edges of the burned area (NR), and then moving on to areas directly outside the mapped burned area (EDG) and finally to areas not at all affected by the fire (UNB).

In HR areas, the fire struck with higher severity, essentially causing the immediate death of a large portion of the above-ground parts of plants. Delayed tree mortality was not detected during the field surveys on HR plots (Figure 10).
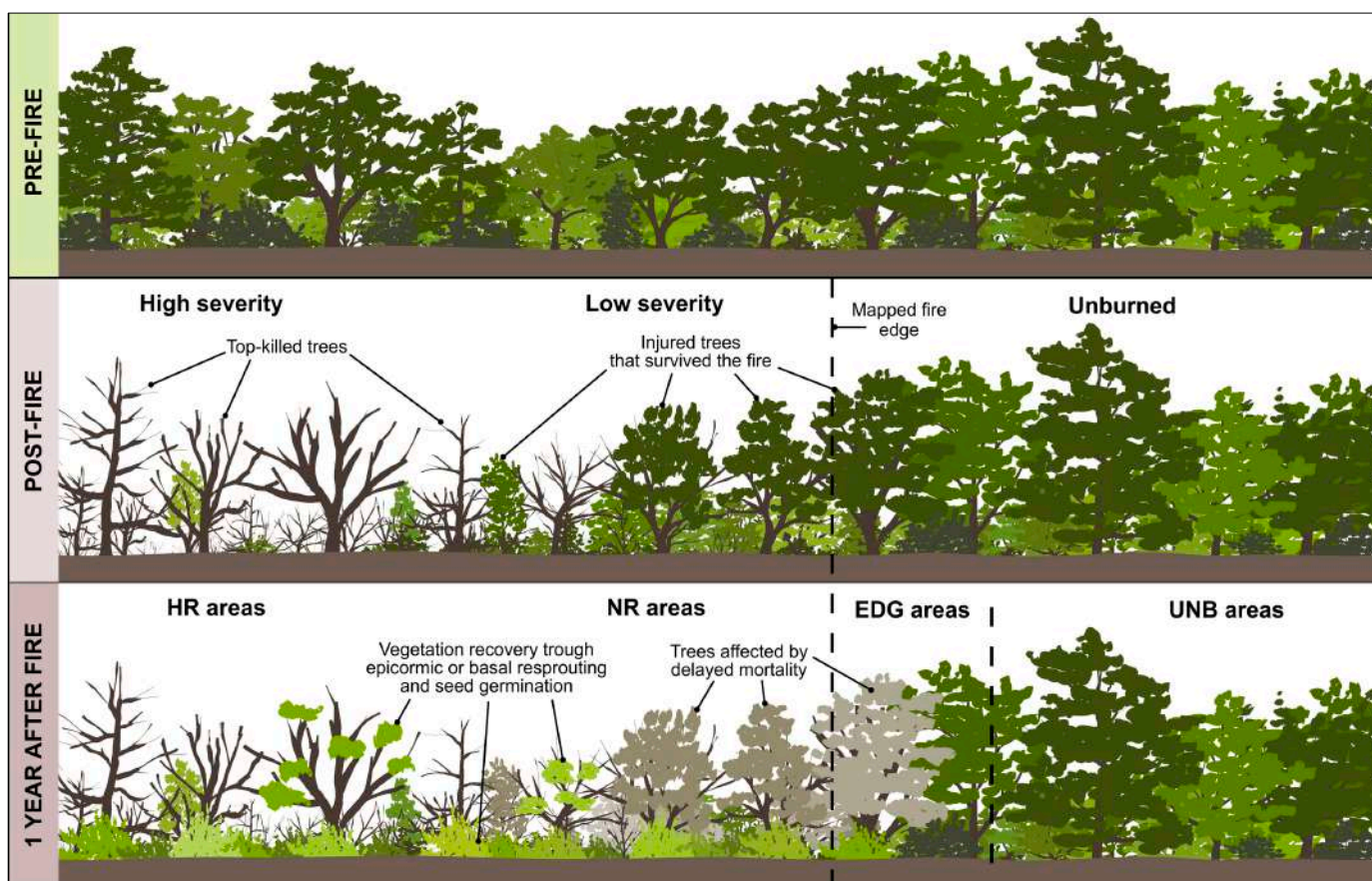
Figure 10. A scheme summarizing the vegetation recovery patterns and delayed tree mortality across the edge of the fire in the investigated woodlands. In areas affected by high-severity fires, most of the plants were immediately top-killed, while, in areas affected by low-severity fires near the fire edge, more plants survived the fire, albeit affected by heat injuries. During the first year after the fire, vegetation recovery occurred through different strategies, such as epicormic resprouting, basal resprouting, and seed germination. However, particularly near the edges of the burned area, delayed mortality affected a percentage of the trees injured by the fire.

On the other hand, in NR areas, the fire struck with lower severity, initially allowing many trees to survive. Afterward, the direct and indirect effects of the fire led to the delayed mortality of a fraction of the surviving trees (Figure 10). This explains why positive values

of NBR$_{post-1yr}$ were detected one year after the fire in the NR areas of the woodlands. The cover and percentage of surviving trees in the NR and HR plots were similar, indicating that delayed tree mortality may cause the substantial loss of the above-ground phytomass, which can match or even exceed the sudden effects of the fire. This is consistent with Reilly and collaborators [35] regarding fires that occurred in the USA, as they found that the total area initially classified as unburned or of very low severity declined by around 38% and often persisted in smaller, more fragmented patches because of delayed mortality. Therefore, declines can also affect the small unburned islands within the fire perimeters. These areas were not investigated in the field because their size did not permit the use of control plots nearby in the unburned area; however, many NBR decline patches were found at the edges of these unburned islands.

The reason that delayed tree mortality was not detected in HR plots, where the injured trees were still alive during the field surveys, could be explained by the mechanism of reduced competition. In fact, a fire reduces the tree density and competition from neighboring trees, herbs, and shrubs, thus increasing the space and resource availability for surviving trees; this may compensate for the immediate effects of the fire, giving injured trees a greater opportunity to survive in the short and mid-term after the fire [2,5,68–70]. Conversely, in NR areas, immediately after the fire, the density of surviving trees was higher; thus, the competition among neighboring plants was stronger than in HR areas, fostering the delayed mortality of the most stressed trees. Another possible explanation could be related to bark beetles' attacks. After a fire, bark beetles may prefer trees with intermediate levels of damage to the crown and cambium [5,71], thus accelerating death in trees affected by low-severity fires.

Although delayed mortality was not detected in HR plots, it cannot be excluded that trees classified as dead immediately after the fire were actually trees that died at a later time. In NR areas, delayed mortality may have occurred even later, making it easier to classify trees affected by delayed mortality.

In terms of resprouting and seed germination, no differences were found between HR and NR plots, suggesting that, even though NBR recovery appeared lower in NR plots, the vegetation regrowth measured in the field was similar to HR plots. Therefore, the lower NBR recovery in NR areas was mainly due to delayed mortality, which counterbalanced the phytomass regeneration based on resprouting and seed germination. In some places, the phytomass loss due to delayed mortality exceeded the new phytomass regenerated by resprouting and seed germination, leading to positive values of dNBR$_{post-1yr}$.

EDG plots, which were outside the burned area mapped immediately after the fire extinction date, were actually affected by the fire to some extent, showing some cases of delayed tree mortality as well. Nevertheless, EDG plots were mostly similar to UNB plots, showing that the Sentinel-2-derived data were not significantly affected by errors due to the image resolution, illumination angles, shadows, or other types of computation errors.

Figure 10 summarizes the observed patterns of vegetation recovery across the edges of the wildfire in the investigated woodlands.

5. Conclusions

The edges of burned areas have been rarely studied so far, particularly in the Mediterranean context, despite their ecological importance at the species, community, ecosystem, and landscape levels. This is partly due to the difficulty in delineating fire edges, caused by technical challenges in defining the fire perimeter. This is particularly true for large fires, which often have extensive marginal areas and may contain unburned islands within them, and in all cases where resorting to remote sensing techniques to map burned areas is an obligatory choice. Therefore, the results of this study may have broad relevance across various contexts.

This study focused on the post-fire vegetation recovery patterns along the edges of a large wildfire in a typical Mediterranean agro-sylvo-pastoral landscape. Specifically, we

analyzed areas experiencing NBR decline one year after the fire, which were typically small and localized near the edges of the burned area.

The study began with the spectral analysis of the vegetation recovery, followed by vegetation surveys conducted in the field to confirm the NBR decline within the areas of interest. These areas were compared with regions showing high NBR recovery and control areas located outside the burned area. It is important to consider that the large size of the total burned area in our case study allowed for the comparison of a representative number of sites with different NBR recovery rates, which might not have been feasible in smaller fires.

Our findings indicate that delayed tree mortality is a significant factor contributing to NBR decline in areas affected by low-severity fires near the edges of the burned area. Even in Mediterranean woodlands, delayed tree mortality is a significant factor that could exacerbate the damage caused by a fire to vegetation, even in areas classified as low severity in the immediate post-fire scenario. This highlights the importance of assessing the long-term effects of a fire [26,33] and underscores the necessity of guiding post-fire restoration activities, such as managing ecological refugia identified in the vicinity of the burned area and within small unburned patches within the fire perimeter. In fact, even if our study primarily focused on a narrow band along the edges of the burned area, delayed mortality events also occurred in unburned or less severely burned patches within the main fire perimeter. Consequently, delayed mortality may become more pronounced in the coming years, as this phenomenon often persists in the years following a fire [35]. Therefore, forests near the edges of burned areas should be treated differently in post-fire management programs.

Given that unburned patches and vegetation around the edges can significantly influence succession processes and vegetation dynamics [28], further analysis is needed to determine whether the observed pattern of vegetation recovery and delayed mortality is consistent across different forest types and species compositions.

References

1. Bowman, D.M.; Balch, J.K.; Artaxo, P.; Bond, W.J.; Carlson, J.M.; Cochrane, M.A.; D'Antonio, C.M.; DeFries, R.S.; Doyle, J.C.; Harrison, S.P. Fire in the Earth system. *Science* **2009**, *324*, 481–484. [CrossRef] [PubMed]
2. Bär, A.; Michaletz, S.T.; Mayr, S. Fire effects on tree physiology. *New Phytol.* **2019**, *223*, 1728–1741. [CrossRef] [PubMed]
3. Robbins, Z.J.; Loudermilk, E.L.; Reilly, M.J.; O'Brien, J.J.; Jones, K.; Gerstle, C.T.; Scheller, R.M. Delayed fire mortality has long-term ecological effects across the Southern Appalachian landscape. *Ecosphere* **2022**, *13*, 1–11. [CrossRef]
4. Sayedi, S.S.; Abbott, B.W.; Vannière, B.; Leys, B.; Colombaroli, D.; Romera, G.G.; Słowiński, M.; Aleman, J.C.; Blarquez, O.; Feurdean, A.; et al. Assessing changes in global fire regimes. *Fire Ecol.* **2024**, *20*, 18. [CrossRef]
5. Hood, S.M.; Varner, J.M.; van Mantgem, P.; Cansler, C.A. Fire and tree death: Understanding and improving modeling of fire-induced tree mortality. *Environ. Res. Lett.* **2018**, *13*, 113004. [CrossRef]
6. Agbeshie, A.A.; Abugre, S.; Atta-Darkwa, T.; Awuah, R. A review of the effects of forest fire on soil properties. *J. For. Res.* **2022**, *33*, 1419–1441. [CrossRef]
7. Pinto-Correia, T.; Vos, W. Multifunctionality in Mediterranean landscapes: Past and future. In *The New Dimensions of the European Landscapes*; Jongman, R.H.G., Ed.; Springer: Wageningen, The Netherlands, 2004; Volume 4, pp. 135–164.
8. Caballero, R. High nature value (HNV) grazing systems in Europe: A link between biodiversity and farm economics. *Open Agric. J.* **2007**, *1*, 1–19. [CrossRef]
9. Rossetti, I.; Bagella, S.; Cappai, C.; Caria, M.C.; Lai, R.; Roggero, P.P.; Martins da Silva, P.; Sousa, J.P.; Querner, P.; Seddaiu, G. Isolated cork oak trees affect soil properties and biodiversity in a Mediterranean wooded grassland. *Agric. Ecosyst. Environ.* **2015**, *202*, 203–216. [CrossRef]
10. Pausas, J.G. Resprouting of Quercus suber in NE Spain after fire. *J. Veg. Sci.* **1997**, *8*, 703–706. [CrossRef]
11. de Villalobos, A.E.; Peláez, D.V.; Bóo, R.M.; Mayor, M.D.; Elia, O.R. Effect of high temperatures on seed germination of Prosopis caldenia Burk. *J. Arid Environ.* **2002**, *52*, 371–378. [CrossRef]
12. Bekdouche, F.; Sahnoune, M.; Krouchi, F.; Achour, S.; Guemati, N.; Derridj, A. The contribution of legumes to post-fire regeneration of *Quercus suber* and *Pinus halepensis* forests in Northeastern Algeria. *Rev. Ecol.* **2011**, *66*, 29–42. [CrossRef]
13. Burrows, G.E.; Chisnall, L.K. Buds buried in bark: The reason why *Quercus suber* (cork oak) is an excellent post-fire epicormic resprouter. *Trees* **2016**, *30*, 241–254. [CrossRef]
14. Cruz, Ó.; García-Duro, J.; Riveiro, S.F.; García-García, C.; Casal, M.; Reyes, O. Fire Severity Drives the Natural Regeneration of *Cytisus scoparius* L. (Link) and *Salix atrocinerea* Brot. Communities and the Germinative Behaviour of These Species. *Forests* **2020**, *11*, 124. [CrossRef]
15. Huerta, S.; Marcos, E.; Fernández-García, V.; Calvo, L. Resilience of Mediterranean communities to fire depends on burn severity and type of ecosystem. *Fire Ecol.* **2022**, *18*, 28. [CrossRef]
16. Rossetti, I.; Cogoni, D.; Calderisi, G.; Fenu, G. Short-Term Effects and Vegetation Response after a Megafire in a Mediterranean Area. *Land* **2022**, *11*, 2328. [CrossRef]
17. de Rigo, D.; Libertà, G.; Houston Durrant, T.; Artés Vivancos, T.; San-Miguel-Ayanz, J. *Forest Fire Danger Extremes in Europe Under Climate Change: Variability and Uncertainty*; Publication Office of the European Union: Luxemburg, 2017.
18. Nolè, A.; Rita, A.; Spatola, M.F.; Borghetti, M. Biogeographic variability in wildfire severity and post-fire vegetation recovery across the European forests via remote sensing-derived spectral metrics. *Sci. Total Environ.* **2022**, *823*, 153807. [CrossRef] [PubMed]
19. Xofis, P.; Buckley, P.G.; Takos, I.; Mitchley, J. Long Term Post-Fire Vegetation Dynamics in North-East Mediterranean Ecosystems. The Case of Mount Athos Greece. *Fire* **2021**, *4*, 92. [CrossRef]
20. El Garroussi, S.; Di Giuseppe, F.; Barnard, C. Europe faces up to tenfold increase in extreme fires in a warming climate. *npj Clim. Atmos. Sci.* **2024**, *7*, 30. [CrossRef]
21. Rodrigues, M.; de la Riva, J.; Domingo, D.; Lamelas, T.; Ibarra, P.; Hoffrén, R.; García-Martín, A. An empirical assessment of the potential of post-fire recovery of tree-forest communities in Mediterranean environments. *For. Ecol. Manag.* **2024**, *552*, 121587. [CrossRef]
22. Miller, J.D.; Knapp, E.E.; Key, C.H.; Skinner, C.N.; Isbell, C.J.; Creasy, R.M.; Sherlock, J.W. Calibration and validation of the relative differenced Normalized Burn Ratio (RdNBR) to three measures of fire severity in the Sierra Nevada and Klamath Mountains, California, USA. *Remote Sens. Environ.* **2009**, *113*, 645–656. [CrossRef]
23. Llorens, R.; Sobrino, J.A.; Cristina Fernández, C.; Fernández-Alonso, J.M.; Vega, J.A. A methodology to estimate forest fires burned areas and burn severity degrees using Sentinel-2 data. Application to the October 2017 fires in the Iberian Peninsula. *Int. J. Appl. Earth Obs. Geoinf.* **2021**, *95*, 1–9. [CrossRef]
24. Gibson, R.K.; White, L.A.; Hislop, S.; Nolan, R.H.; Dorrough, J. The post-fire stability index; a new approach to monitoring post-fire recovery by satellite imagery. *Remote Sens. Environ.* **2022**, *280*, 113151. [CrossRef]
25. Laneve, G.; Di Fonzo, M.; Pampanoni, V.; Bueno Morles, R. Progress and Limitations in the Satellite-Based Estimate of Burnt Areas. *Remote Sens.* **2024**, *16*, 42. [CrossRef]
26. Key, C.H. Ecological and sampling constraints on defining landscape fire severity. *Fire Ecol.* **2006**, *2*, 34–59. [CrossRef]
27. Verbyla, D.L.; Kasischke, E.S.; Hoy, E.E. Seasonal and topographic effects on estimating fire severity from landsat TM/ETM+ data. *Int. J. Wildland Fire* **2008**, *17*, 527–534. [CrossRef]
28. Kolden, C.A.; Lutz, J.A.; Key, C.H.; Kane, J.T.; van Wagtendonk, J.W. Mapped versus actual burned area within wildfire perimeters: Characterizing the unburned. *For. Ecol. Manag.* **2012**, *286*, 38–47. [CrossRef]

29. Greene, D.F.; Macdonald, S.E.; Cumming, S.; Swift, L. Seedbed variation from the interior through the edge of a large wildfire in Alberta. *Can. J. For. Res.* **2005**, *35*, 1640–1647. [CrossRef]

30. Harper, K.A.; Drapeau, P.; Lesieur, D.; Bergeron, Y. Forest structure and composition at fire edges of different ages: Evidence of persistent structural features on the landscape. *For. Ecol. Manag.* **2014**, *314*, 131–140. [CrossRef]

31. Stevens-Rumann, C.S.; Prichard, S.J.; Strand, E.K.; Morgan, P. Prior wildfires influence burn severity of subsequent large fires. *Can. J. For. Res.* **2016**, *46*, 1375–1385. [CrossRef]

32. Zhang, X.; Fan, J.; Zhou, J.; Gui, L.; Bi, Y. Mapping Fire Severity in Southwest China Using the Combination of Sentinel 2 and GF Series Satellite Images. *Sensors* **2023**, *23*, 2492. [CrossRef]

33. Key, C.H.; Benson, N.C. Landscape Assessment (LA) Sampling and Analysis Methods. In *FIREMON: Fire Effects Monitoring and Inventory System*; USDA Forest Service, Rocky Mountain Research Station: Ogden, UT, USA, 2006.

34. Larrivée, M.; Drapeau, P.; Fahrig, L. Edge effects created by wildfire and clear-cutting on boreal forest ground-dwelling spiders. *For. Ecol. Manag.* **2008**, *255*, 1434–1445. [CrossRef]

35. Reilly, M.J.; Zuspan, A.; Yang, Z. Characterizing post-fire delayed tree mortality with remote sensing: Sizing up the elephant in the room. *Fire Ecol.* **2023**, *19*, 64. [CrossRef]

36. Diffendorfer, J.; Fleming, G.M.; Tremor, S.; Spencer, W.; Beyers, J.L. The role of fire severity, distance from fire perimeter and vegetation on post-fire recovery of small-mammal communities in chaparal. *Int. J. Wildland Fire* **2012**, *21*, 436–448. [CrossRef]

37. Román-Cuesta, R.M.; Gracia, M.; Retana, J. Factors influencing the formation of unburned forest islands within the perimeter of a large forest fire. *For. Ecol. Manag.* **2009**, *258*, 71–80. [CrossRef]

38. Kane, V.R.; North, M.P.; Lutz, J.A.; Churchill, D.J.; Roberts, S.L.; Smith, D.F.; McGaughey, R.J.; Kane, J.T.; Brooks, M.L. Assessing fire effects on forest spatial structure using a fusion of Landsat and airborne LiDAR data in Yosemite National Park. *Remote Sens. Environ.* **2014**, *151*, 89–101. [CrossRef]

39. Meddens, A.J.H.; Kolden, C.A.; Lutz, J.A.; Abatzoglou, J.T.; Hudak, A.T. Spatiotemporal patterns of unburned areas within fire perimeters in the northwestern United States from 1984 to 2014. *Ecosphere* **2018**, *9*, e02029. [CrossRef]

40. Linley, G.D.; Jolly, C.J.; Doherty, T.S.; Geary, W.L.; Armenteras, D.; Belcher, C.M.; Bliege Bird, R.; Duane, A.; Fletcher, M.-S.; Giorgis, M.A.; et al. What do you mean, 'megafire'? *Glob. Ecol. Biogeogr.* **2022**, *31*, 1906–1922. [CrossRef]

41. Stoof, C.R.; De Vries, J.R.; Castellnou Ribau, M.; Fernández, M.F.; Flores, D.; Galarza Villamar, J.; Kettridge, N.; Lartey, D.; Moore, P.F.; Newman Thacker, F.; et al. Megafire: An Ambiguous and Emotive Term Best Avoided by Science. *Glob. Ecol. Biogeogr.* **2024**, *33*, 341–351. [CrossRef]

42. Carmignani, L.; Oggiano, G.; Funedda, A.; Conti, P.; Pasci, S.; Barca, S. *Carta Geologica della Sardegna*; Litografia Artistica Cartografica: Florence, Italy, 2008.

43. Rivas-Martínez, S.; Rivas-Saenz, S. Worldwide bioclimatic classification system. *Glob. Geobot.* **2011**, *1*, 1–634. [CrossRef]

44. Regione Autonoma della Sardegna (RAS). Available online: https://www.sardegnageoportale.it/ (accessed on 6 March 2023).

45. Copernicus Sentinel Data 2021 and 2022. Available online: https://scihub.copernicus.eu/ (accessed on 20 August 2022).

46. European Forest Fire Information System (EFFIS). Available online: https://effis.jrc.ec.europa.eu/about-effis/technical-background/rapid-damage-assessment (accessed on 20 August 2022).

47. QGIS Development Team. QGIS Geographic Information System. *Open Source Geospatial Foundation Project.* 2023. Available online: http://qgis.osgeo.org (accessed on 6 March 2023).

48. *JASP*, version 0.18.1; University of Amsterdam: Amsterdam, The Netherlands, 2023.

49. Fernández-Guisuraga, J.M.; Fernandes, P.M.; Tárrega, R.; Beltrán-Marcos, D.; Calvo, L. Vegetation recovery drivers at short-term after fire are plant community-dependent in mediterranean burned landscapes. *For. Ecol. Manag.* **2023**, *539*, 121034. [CrossRef]

50. D'Odorico, P.; Okin, G.S.; Bestelmeyer, B.T. A synthetic review of feedbacks and drivers of shrub encroachment in arid grasslands. *Ecohydrology* **2012**, *5*, 520–530. [CrossRef]

51. Deák, B.; Valkó, O.; Török, P.; Végvári, Z.; Härtel, T.; Schmotzer, A.; Kapocsi, I.; Tóthmérész, B. Grassland fires in Hungary—Experiences of nature conservationists on the effects of fire on biodiversity. *Appl. Ecol. Environ. Res.* **2014**, *12*, 267–283. [CrossRef]

52. Fultz, L.M.; Moore-Kucera, J.; Dathe, J.; Davinic, M.; Perry, G.; Wester, D.; Schwilk, D.W.; Rideout-Hanzak, S. Forest wildfire and grassland prescribed fire effects on soil biogeochemical processes and microbial communities: Two case studies in the semiarid Southwest. *Appl. Soil Ecol.* **2016**, *99*, 118–128. [CrossRef]

53. Yan, H.; Liu, G. Fire's Effects on Grassland Restoration and Biodiversity Conservation. *Sustainability* **2021**, *13*, 12016. [CrossRef]

54. Wang, G.; Li, J.; Ravi, S.; Theiling, B.; Burger, W. Fire changes the spatial pattern and dynamics of soil nitrogen (N) and $\delta 15N$ at a grassland-shrubland ecotone. *J. Arid Environ.* **2021**, *186*, 104422. [CrossRef]

55. Stambaugh, M.C.; Hammer, L.D.; Godfrey, R. Performance of burn-severity metrics and classification in oak woodlands and grasslands. *Remote Sens.* **2015**, *7*, 10501–10522. [CrossRef]

56. Stavi, I. Wildfires in Grasslands and Shrublands: A Review of Impacts on Vegetation, Soil, Hydrology, and Geomorphology. *Water* **2019**, *11*, 1042. [CrossRef]

57. Das, A.J.; Stephenson, N.L.; Davis, K.P. Why do trees die? Characterizing the drivers of background tree mortality. *Ecology* **2016**, *97*, 2616–2627. [CrossRef]

58. Pausas, J.G.; Vallejo, V.R. The role of fire in European Mediterranean ecosystems. In *Remote Sensing of Large Wildfires in the European Mediterranean Basin*; Chuvieco, E., Ed.; Springer: Berlin, Germany, 1999; pp. 3–16. [CrossRef]

59. Rulli, M.C.; Offeddu, L.; Santini, M. Modeling post-fire water erosion mitigation strategies. *Hydrol. Earth Syst. Sci.* **2013**, *17*, 2323–2337. [CrossRef]

60. Alarcon-Aguirre, G.; Miranda Fidhel, R.F.; Ramos Enciso, D.; Canahuire-Robles, R.; Rodriguez-Achata, L.; Garate-Quispe, J. Burn Severity Assessment Using Sentinel-1 SAR in the Southeast Peruvian Amazon, a Case Study of Madre de Dios. *Fire* **2022**, *5*, 94. [CrossRef]

61. Reinhardt, E.D.; Keane, R.E.; Brown, J.K. Modeling fire effects. *Int. J. Wildland Fire* **2001**, *10*, 373–380. [CrossRef]

62. Reinhardt, E.D.; Dickinson, M.B. First-Order Fire Effects Models for Land Management: Overview and Issues. *Fire Ecol.* **2010**, *6*, 131–142. [CrossRef]

63. Michaletz, S.T. Xylem dysfunction in fires: Towards a hydraulic theory of plant responses to multiple disturbance stressors. *New Phytol.* **2018**, *217*, 1391–1393. [CrossRef]

64. Barker, J.S.; Gray, A.N.; Fried, J.S. The Effects of Crown Scorch on Post-fire Delayed Mortality Are Modified by Drought Exposure in California (USA). *Fire* **2022**, *5*, 21. [CrossRef]

65. Kane, J.M.; van Mantgem, P.J.; Lalemand, L.B.; Keifer, M. Higher sensitivity and lower specificity in post-fire mortality model validation of 11 western US tree species. *Int. J. Wildland Fire* **2017**, *26*, 444–454. [CrossRef]

66. van Mantgem, P.J.; Stephenson, N.L.; Knapp, E.; Battles, J.; Keeley, J.E. Long-term effects of prescribed fire on mixed conifer forest structure in the Sierra Nevada, California. *For. Ecol. Manag.* **2011**, *261*, 989–994. [CrossRef]

67. Maringer, J.; Ascoli, D.; Küffer, N.; Schmidtlein, S.; Conedera, M. What drives European beech (*Fagus sylvatica* L.) mortality after forest fires of varying severity? *For. Ecol. Manag.* **2016**, *368*, 81–93. [CrossRef]

68. Battipaglia, G.; Savi, T.; Ascoli, D.; Castagneri, D.; Esposito, A.; Mayr, S.; Nardini, A. Effects of prescribed burning on ecophysio-logical, anatomical and stem hydraulic properties in *Pinus pinea* L. Tree Physiol. **2016**, *36*, 1–13. [CrossRef] [PubMed]

69. Valor, T.; González-Olabarria, J.R.; Piqué, M. Assessing the impact of prescribed burning on the growth of European pines. *For. Ecol. Manag.* **2015**, *343*, 101–109. [CrossRef]

70. Alfaro-Sánchez, R.; Julio Camarero, J.; Sánchez-Salguero, R.; Sangüesa-Barreda, G.; De Las Heras, J. Post-fire Aleppo pine growth, C and N isotope composition depend on site dryness. *Trees* **2016**, *30*, 581–595. [CrossRef]

71. Jenkins, M.J.; Runyon, J.B.; Fettig, C.J.; Page, W.G.; Bentz, B.J. Interactions among the mountain pine beetle, fires, and fuels. *For. Sci.* **2014**, *60*, 489–501. [CrossRef]